Divergent thermal expansion and Grüneisen ratio in a quadrupolar Kondo metal

A. Wörl, M. Garst, Y. Yamane, S. Bachus, T. Onimaru, Philipp Gegenwart

Angaben zur Veröffentlichung / Publication details:

Wörl, A., M. Garst, Y. Yamane, S. Bachus, T. Onimaru, and Philipp Gegenwart. 2022. "Divergent thermal expansion and Grüneisen ratio in a quadrupolar Kondo metal." *Physical Review Research* 4 (2): L022053. https://doi.org/10.1103/physrevresearch.4.l022053.

Letter

Divergent thermal expansion and Grüneisen ratio in a quadrupolar Kondo metal

A. Wörl [1,*] M. Garst [2,3] Y. Yamane [4,†] S. Bachus [1] T. Onimaru [4] and P. Gegenwart [1,‡]

[1]*Experimental Physics VI, Center for Electronic Correlations and Magnetism, University of Augsburg, 86159 Augsburg, Germany*

[2]*Institute for Theoretical Solid State Physics, Karlsruhe Institute of Technology, 76131 Karlsruhe, Germany*

[3]*Institute for Quantum Materials and Technology, Karlsruhe Institute of Technology, 76131 Karlsruhe, Germany*

[4]*Department of Quantum Matter, Graduate School of Advanced Science and Engineering, Hiroshima University, Higashi-Hiroshima 739-8530, Japan*

(Received 28 July 2021; revised 21 April 2022; accepted 26 April 2022; published 6 June 2022)

We report on the low-temperature thermal expansion and magnetostriction of the single-impurity quadrupolar Kondo candidate $Y_{1-x}Pr_xIr_2Zn_{20}$. In the dilute limit, we find a quadrupolar strain that possesses a singular dependence on temperature T, $\varepsilon_u \sim H^2 \log(1/T)$, for a small but finite magnetic field H. Together with the previously reported anomalous specific heat C, this implies a quadrupolar Grüneisen ratio $\Gamma_u = \partial_T \varepsilon_u / C \sim H^2/[T^2 \log(1/T)]$ whose divergence for finite H is consistent with the scenario of a quadrupolar Kondo effect. In addition, we find a singular behavior of the isotropic strain ε_B in zero magnetic field resulting in a divergence of both the volume thermal expansion and the volume Grüneisen parameter. We speculate that this behavior might be also induced by putative Kondo correlations via elastic anharmonicities or static strain disorder.

DOI: 10.1103/PhysRevResearch.4.L022053

In solid state physics, non-Fermi liquid phases describe unconventional metallic states of matter. Such exotic phases have been extensively studied in the framework of heavy fermion (HF) quantum criticality [1]. A magnetic quantum critical point typically forms in Ce- and Yb-based intermetallic systems that are located in between a Kondo screened Fermi liquid and a long range antiferromagnetically ordered state. The divergence of the Grüneisen parameter, defined as the ratio of volume thermal expansion to specific heat, is a universal signature of pressure sensitive quantum critical points [2,3].

In addition, there has been a particular focus on exploring non-Fermi liquid states that are related to electric quadrupole moments and on identifying potential links between these states and magnetic HF quantum criticality [4–7]. Quadrupolar ground states form, for instance, in non-Kramers Pr- and U-based intermetallics, given that certain symmetry constraints are fulfilled. A possible cause for unconventional metallic behavior in these materials is the quadrupolar Kondo effect, which was postulated by Cox in 1987 [8]. Here, the simultaneous overscreening of a localized quadrupole moment by two channels of conduction electrons, which are related to their spin degree of freedom, leads to non-Fermi liquid behavior in specific heat [$C/T \sim \log(1/T)$], electrical resisitivity ($\rho/\rho_0 \sim 1 + A\sqrt{T}$), and quadrupole susceptibility [$\chi_Q \sim \log(1/T)$] as well as an unconventional residual entropy of $S = R \log \sqrt{2}$ [9].

Cubic Pr-based 1-2-20 systems are prototypical to study such novel quadrupolar [10,11] as well as higher multipolar related correlation effects [12–14]. $PrIr_2Zn_{20}$, for instance, has a well defined quadrupolar non-Kramers Γ_3 ground state doublet (point group T_d) [15] and displays clear signatures of the quadrupolar Kondo lattice effect [4], which are cut off by antiferroquadrupolar order at 0.11 K [16]. Recent studies on highly diluted $Y_{1-x}Pr_xIr_2Zn_{20}$ provided direct evidence of the single-impurity quadrupolar Kondo effect, based on characteristic non-Fermi liquid behaviors found in the specific heat, electrical resistivity, and elastic constant [5,17]. Nevertheless, evidence for the residual entropy $S = R \log \sqrt{2}$ remains elusive so far [5].

The concept of the Grüneisen parameter can be generalized to all irreducible representations of elastic strains. Such a generalized Grüneisen parameter is expected to diverge close to a quantum critical point provided that the associated stress couples to a relevant operator of the critical fixed point [2,18]. For the single-impurity quadrupolar Kondo fixed point, this is the case for the quadrupolar stress σ_u, that breaks the cubic symmetry, and, as a consequence, destabilizes the non-Fermi liquid physics and quenches the residual entropy. This implies that the quadrupolar Grüneisen ratio $\Gamma_u = (\partial_T \varepsilon_u)/C$ diverges in a characteristic manner. Here, $\varepsilon_u = (2\varepsilon_{zz} - \varepsilon_{xx} - \varepsilon_{yy})/\sqrt{3}$ is the strain component of the Γ_3 doublet that is conjugate to σ_u with the corresponding thermal expansion $\alpha_u = \partial_T \varepsilon_u$ and $C = C_m/V_m$ the specific heat with the molar volume V_m and the molar specific heat C_m. Using a thermodynamic identity, $\Gamma_u = -1/T(dT/d\sigma_u)_S$ also quantifies the adiabatic change of temperature upon the variation of σ_u and thus describes an elastocaloric effect [19].

*andreas.woerl@physik.uni-augsburg.de

†Present address: Department of Material Science, Graduate School of Science, University of Hyogo, Kamigori, Hyogo 678-1297, Japan.

‡philipp.gegenwart@physik.uni-augsburg.de

The application of a magnetic field $\boldsymbol{H}$ will split the non-Kramers Γ_3 doublet resulting in a finite quadrupole moment $\langle Q\rangle \sim \chi_Q H^2$ of each Pr^{3+} ion, that is proportional to H^2 for small fields due to time-reversal symmetry. This induces a local quadrupolar strain via the elastic coupling g_{Γ_3}, and after averaging over Pr disorder results in a homogeneous strain $\varepsilon_u \sim g_{\Gamma_3} n_{Pr} \chi_Q H^2/c_u$ where n_{Pr} is the Pr^{3+} density and $c_u = (c_{11} - c_{12})/2$ the corresponding elastic constant. The quadrupolar Kondo effect predicts $\chi_Q \sim \log(1/T)$ resulting in a singular temperature dependence of the quadrupolar strain $\varepsilon_u \sim n_{Pr} H^2 \log(1/T)$. Finally, using that the specific heat at low temperatures is dominated by the contribution of the Pr^{3+} ions, $C_m \sim n_{Pr} T \log(1/T)$ for small magnetic fields [5], one expects for the quadrupolar Grüneisen parameter $\Gamma_u \sim H^2/[T^2 \log(1/T)]$. Consequently, thermal expansion and magnetostriction experiments are ideally suited for the investigation of the non-Fermi liquid behavior associated with the quadrupolar Kondo effect.

In this work, we perform such measurements on highly diluted single crystalline $Y_{1-x}Pr_xIr_2Zn_{20}$. As our key finding, we confirm experimentally that the temperature dependence for the quadrupolar strain ε_u and the associated quadrupolar Grüneisen parameter Γ_u is indeed consistent with the suggested quadrupolar Kondo scenario [5,17]. Remarkably, we also find that the volume strain ε_B shows a similar singular behavior in zero magnetic field although isotropic stress does not directly couple to a relevant operator of the quadrupolar Kondo fixed point. We speculate that an indirect coupling might be generated either by elastic anharmonicities or by static strain disorder accounting for the experimentally observed divergence in the volume thermal expansion.

Ultrahigh-resolution thermal expansion and magnetostriction measurements were carried out in a dilution refrigerator using a miniaturized capacitive dilatometer [20]. Central to this study is a highly diluted $Y_{1-x}Pr_xIr_2Zn_{20}$ single crystal with $x = 0.036$, for which relative length changes were measured along a cubic $\langle 100\rangle$ direction, with magnetic fields applied either parallel or perpendicular to the measurement direction. The magnetic field direction is defined as [001] in the following, so that ε_{zz} and ε_{xx} correspond to longitudinal $\varepsilon_\parallel$ and transverse strain $\varepsilon_\perp$, respectively. As the applied field does not break the symmetry within the (x, y) plane, we can assume that $\varepsilon_{xx} = \varepsilon_{yy}$. The measurement of longitudinal and transverse strain in magnetic field then allows one to infer the values of the isotropic strain $\varepsilon_B = \varepsilon_{xx} + \varepsilon_{yy} + \varepsilon_{zz}$ and the quadrupolar strain ε_u, as detailed in the Supplemental Material (SM) [21]. An unavoidable side effect of the experimental technique is a small force of approximately 4 N [20] acting on the sample along the measurement direction, which corresponds to a tiny uniaxial stress of a few MPa. To clarify whether this effect has an impact on the deduced relative length changes, we performed complementary measurements on a [111] oriented single crystal with a comparable Pr concentration of $x = 0.033$. For further characterization, a special uniaxial stress capacitive dilatometer [27], that exerts a roughly 15 times larger force on the sample than the miniaturized dilatometer, was employed. For details on the single crystalline samples examined in this study, see SM [21].

First, we discuss the quadrupolar thermal expansion coefficient $\alpha_u = \partial_T \varepsilon_u$ of $Y_{1-x}Pr_xIr_2Zn_{20}$ with $x = 0.036$. The

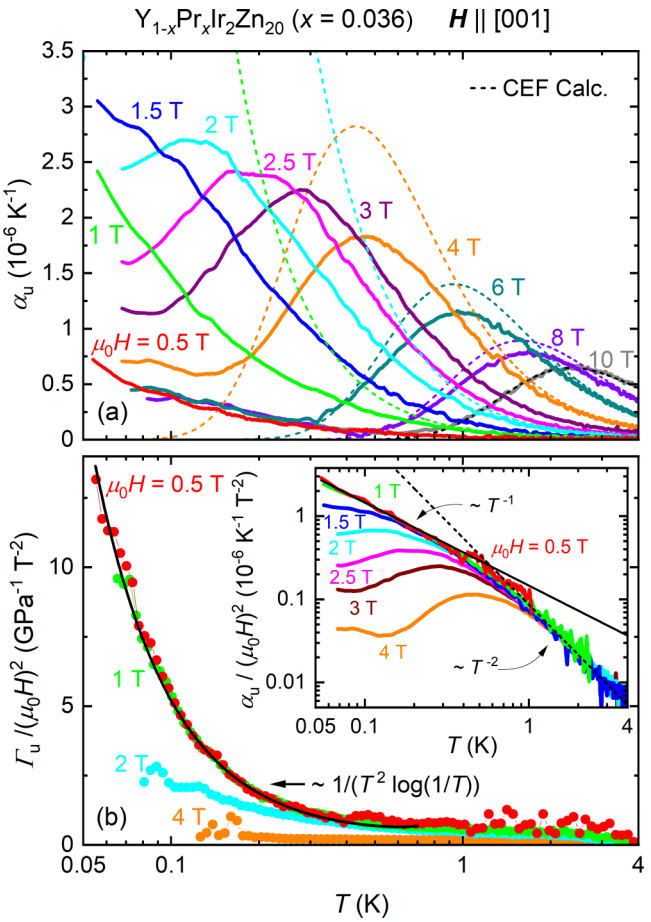

FIG. 1. (a) Temperature dependence of the quadrupolar thermal expansion coefficient α_u at various magnetic fields $\boldsymbol{H} \parallel [001]$. The dashed lines are crystal electric field (CEF) calculations. (b) Quadrupolar Grüneisen parameter normalized to magnetic field Γ_u/H^2 as a function of temperature for $\boldsymbol{H} \parallel [001]$. The black solid line denotes the theoretically expected temperature dependence of Γ_u for the quadrupolar Kondo effect. The inset shows α_u/H^2 vs T on a log-log scale, together with power law divergences as dashed and solid lines.

respective data is derived from the measurement of the longitudinal $\alpha_\parallel$ and the volume thermal expansion β for $\boldsymbol{H} \parallel [001]$ via the the relation $\alpha_u = \sqrt{3}(\alpha_\parallel - \beta/3)$. A detailed derivation of this relation and an overview of the data of $\alpha_\parallel$ and β is provided in the SM [21]. The quadrupolar thermal expansion coefficient α_u is shown in Fig. 1(a) on a logarithmic temperature scale ranging from 0.05 to 4 K for various magnetic fields up to 10 T. For small fields, α_u increases down to lowest temperatures. At around 1.5 T a maximum develops whose position shifts to higher temperatures as a function of increasing field. At the same time, the height of the maximum continuously decreases with H. For $\mu_0 H \gtrsim 8$ T, this peak is quantitatively captured by crystal electric field (CEF) calculations [21] as indicated by the dashed lines.

The ratio $\alpha_u/(\mu_0 H)^2$ is shown in the inset of Fig. 1(b). For temperatures $k_B T \gg \mu_B \mu_0 H$, the data collapses onto a single curve that exhibits a crossover from a $\alpha_u/H^2 \sim \partial_T \chi_Q \sim 1/T$ behavior at low temperature, consistent with the quadrupolar Kondo effect, to a $1/T^2$ dependence at high temperature as

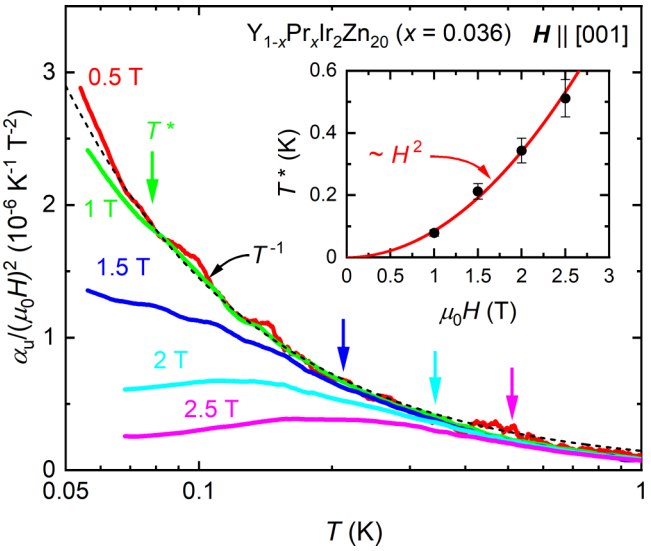

FIG. 2. Quadrupolar thermal expansion coefficient normalized to magnetic field $\alpha_u/(\mu_0 H)^2$ as a function of temperature for magnetic field $\boldsymbol{H} \parallel [001]$. The dashed solid line indicates the T^{-1} single-impurity quadrupole Kondo dependence. Arrows denote a characteristic temperature T^*, below which deviations from the universal single-impurity quadrupole Kondo behavior arise. The inset displays T^* as a function of magnetic field, with the red solid line indicating a H^2 field dependence.

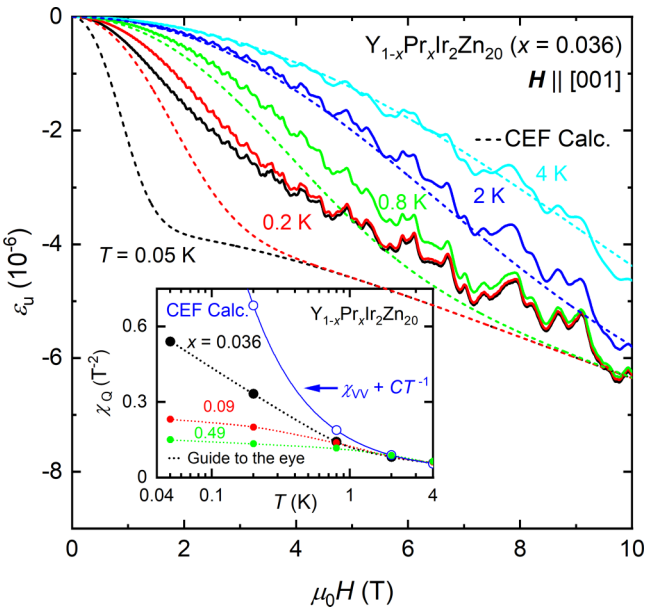

FIG. 3. Magnetic field variation of the quadrupolar magnetostriction ε_u for $\boldsymbol{H} \parallel [001]$ at different temperatures. The dashed lines are CEF calculations. The inset shows the quadrupole susceptibility χ_Q extracted from the quadratic dependence $\varepsilon_u \sim n_{Pr}\chi_Q H^2$ at small H for three different Pr concentrations x. The CEF prediction is shown as a solid blue line, whose temperature dependence is characterized by the superposition of a constant Van Vleck, χ_{VV}, and a C/T Curie contribution which cannot describe the experimental data at low T.

expected for a Curie susceptibility $\chi_Q \sim 1/T$ of a fully localized Γ_3 doublet [21]. The crossover temperature of ~0.6 K is consistent with previous studies [5,17]. By using the molar $4f$ specific heat C_m [21], measured on a single crystal from the same batch with a comparable Pr concentration of $x = 0.044$, we evaluate the quadrupolar Grüneisen parameter that follows the expected singular behavior $\Gamma_u \sim H^2/[T^2 \log(1/T)]$ for low magnetic fields as shown by the black solid line in Fig. 1(b).

Within the framework of the quadrupolar Kondo model, the deviation from the characteristic quadrupole Kondo behavior for larger magnetic fields can be attributed to both a channel and a quadrupolar asymmetry, induced in linear and quadratic order in H, respectively. At small fields, the first effect is expected to dominate and results in a crossover temperature $T^* \sim H^2$ (see Ref. [9]), separating non-Fermi and Fermi liquid behavior. In order to specify the origin of the magnetic field induced crossover in highly diluted $Y_{1-x}Pr_xIr_2Zn_{20}$, Fig. 2 displays the data of $\alpha_u/(\mu_0 H)^2$ on a logarithmic temperature scale at small magnetic fields up to 2.5 T. The crossover temperature T^*, which is determined as the temperature at which deviations from the universal single-impurity quadrupole Kondo behavior arise, is indicated by an arrow for each magnetic field. The inset displays the characteristic temperature T^* as a function of magnetic field, whereby the red solid line indicates a quadratic magnetic field dependence. Indeed, the characteristic temperature T^* estimated from the quadrupolar thermal expansion data can be well scaled with $T^* \sim H^2$. This indicates that the field induced channel asymmetry is the dominating perturbation at low magnetic field leading to the experimentally found deviations from the quadrupole Kondo behavior at low temperature, which is in very good agreement with the theoretical expectation.

The results on the quadrupolar thermal expansion coefficient α_u and the quadrupolar Grüneisen parameter Γ_u, which are indicative of the single-impurity quadrupole Kondo effect, are further corroborated by the quadrupolar magnetostriction ε_u displayed in Fig. 3. The quadrupolar magnetostriction coefficient ε_u is derived from the measurement of the longitudinal $\varepsilon_\parallel$ and the volume magnetostriction coefficient ε_B by using the relation $\varepsilon_u = \sqrt{3}(\varepsilon_\parallel - \varepsilon_B/3)$ for $\boldsymbol{H} \parallel [001]$. The data of $\varepsilon_\parallel$ and ε_B used for the calculation of ε_u is provided in the SM [21]. By analyzing the initial quadratic field dependence of $\varepsilon_u \sim n_{Pr}\chi_Q H^2$ [21], we extract the quadrupolar susceptibility χ_Q that is shown for various Pr doping x in the inset of Fig. 3. The CEF calculation, which predicts a Curie-like $1/T$ temperature dependence on top of a constant Van Vleck contribution, can only capture the behavior of χ_Q at elevated temperature. At low T and for the lowest doping concentration $x = 0.036$ our results are consistent with a logarithmic temperature dependence of χ_Q. For higher doping, the susceptibility is suppressed at low temperatures indicating a quenching of the quadrupolar Kondo effect, likely induced by interactions between Pr^{3+} ions.

We now turn to the discussion of the volume thermal expansion coefficient $\beta = \partial_T \varepsilon_B$. In Fig. 4(a), β is shown for the highly diluted single crystal with $x = 0.036$. Remarkably, the thermal expansion coefficient at zero field increases down to lowest temperatures. This continuous increase is quenched

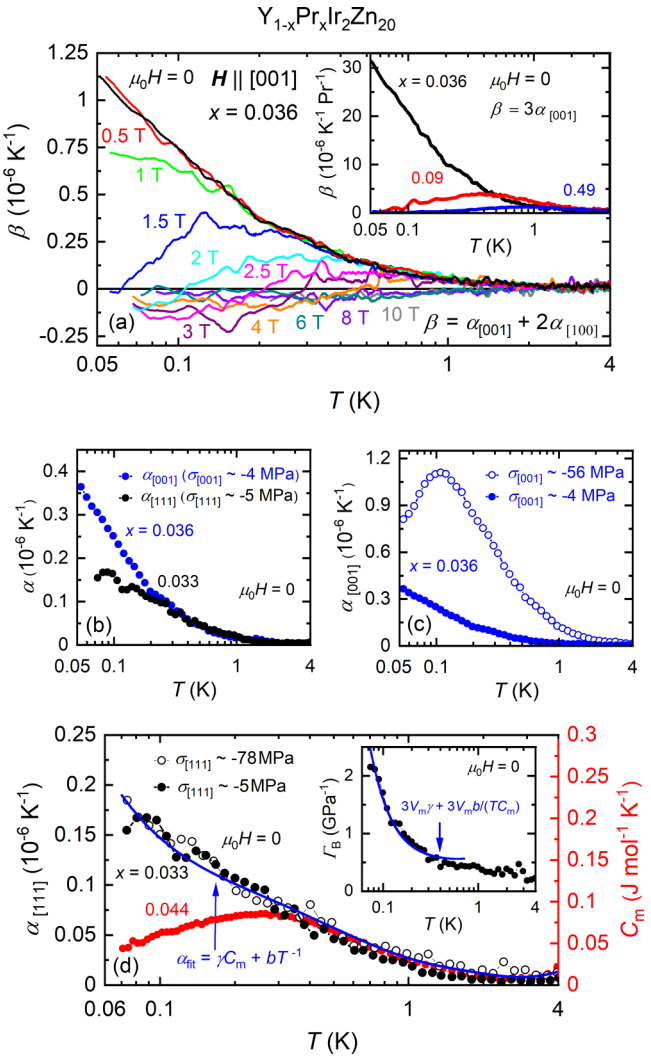

FIG. 4. (a) Volume thermal expansion coefficient β as a function of temperature at various magnetic fields $\boldsymbol{H} \parallel [001]$. The inset shows β at zero magnetic field for three different Pr concentrations x. (b) Temperature dependencies of the uniaxial thermal expansion coefficients $\alpha_{[001]}$ and $\alpha_{[111]}$ measured with the miniaturized dilatometer at zero magnetic field. (c) Temperature dependencies of $\alpha_{[001]}$ measured with the miniaturized (closed circles) and the uniaxial stress dilatometer (open circles). (d) Temperature dependencies of $\alpha_{[111]}$ obtained by the miniaturized (filled circles) and the uniaxial stress dilatometer (open circles) together with specific heat data, partially taken from Ref. [5]. The blue solid line is a fit to $\alpha_{[111]}$ using $\alpha_{\mathrm{fit}} = \gamma C_{\mathrm{m}} + bT^{-1}$. The inset displays the temperature dependence of the bulk Grüneisen parameter Γ_{B}.

by the application of a field and, for $\mu_0 H \gtrsim 6$ T, the volume thermal expansion practically vanishes. Similarly, β is also suppressed by larger doping as shown in the inset for zero field. The continuous increase of β on cooling at zero field and low doping is unexpected at first sight as the influence of the quadrupolar moments should in lowest order average out in the bulk thermal expansion. A parasitic signal could potentially arise from the presence of a small uniaxial stress from the sample holder that is on the order of a few MPa in the case of the miniaturized dilatometer and breaks the isotropy of the environment. In order to clarify this influence, we compare in Fig. 4(b) the uniaxial thermal expansion along crystallographic [001] and [111] directions measured on two single crystals with almost the same doping level. While a uniaxial stress along [111] only activates the bulk strain ε_{B}, a uniaxial stress along [001] induces both bulk and quadrupolar strains where the latter couples linearly to the Γ_3 ground state doublet of the Pr^{3+} ions. At very low temperature, we find indeed a difference between $\alpha_{[001]}$ and $\alpha_{[111]}$ that we attribute to the presence of a small uniaxial stress exerted by the dilatometer.

To demonstrate the tremendous effect of uniaxial stress along [001], we performed a complementary measurement using a uniaxial stress dilatometer with an applied uniaxial stress approximately 15 times larger than in the miniaturized dilatometer [see Fig. 4(c)]. Under higher uniaxial stress, the divergence of $\alpha_{[001]}$ is suppressed and a maximum forms at around 0.11 K, suggesting the breakdown of the two-channel Kondo effect due to the linear in strain splitting of the Γ_3 ground state doublet.

Figure 4(d) displays the temperature dependence of $\alpha_{[111]}$ measured with both the miniaturized and the uniaxial stress dilatometer at zero magnetic field. As there is no notable difference between the two data sets, we conclude that the divergent temperature dependence of $\alpha_{[111]}$ is in fact an intrinsic volume effect and not artificially induced by the uniaxial stress applied externally along the measurement direction. This result is striking as it is markedly different from the molar specific heat of the $4f$ electrons C_{m} as shown by the red symbols. The thermal expansion is well described by a fit $\alpha_{\mathrm{fit}} = \gamma C_{\mathrm{m}} + b/T$ (blue line) that assumes two contributions. The first obeys Grüneisen scaling with a constant γ and the second contribution diverges like $1/T$, which is reminiscent of the behavior of α_{u}/H^2 shown in the inset of Fig. 1(b). Consequently, the bulk Grüneisen ratio $\Gamma_{\mathrm{B}} = V_{\mathrm{m}} 3\alpha_{[111]}/C_{\mathrm{m}} \approx 3V_{\mathrm{m}}\gamma + 3V_{\mathrm{m}} b/(TC_{\mathrm{m}})$ exhibits a divergence as a function of temperature similar to Γ_{u}/H^2 shown in Fig. 1(b).

In the following, we speculate on the origin of this surprising finding of an intrinsic bulk thermal expansion that increases down to lowest temperatures. The elastic coupling g_{Γ_3} to the non-Kramers Γ_3 doublet leads in second order perturbation theory to the following correction to the elastic Hamiltonian:

$$\delta\mathcal{H} = -\frac{g_{\Gamma_3}^2 \chi_{\mathrm{Q}}}{2} \sum_{\alpha} \left[\varepsilon_{\mathrm{u}}^2(\vec{r}_\alpha) + \varepsilon_{\mathrm{v}}^2(\vec{r}_\alpha)\right]. \tag{1}$$

Here, $\varepsilon_{\mathrm{u/v}}(\vec{r}_\alpha)$ are the two components of the local quadrupolar strain doublet at the position $\vec{r}_\alpha$ of the Pr^{3+} ion with index α. After averaging over Pr disorder this Hamiltonian recovers the renormalization of the quadrupolar elastic constant $\delta c_{\mathrm{u}} = -n_{\mathrm{Pr}} g_{\Gamma_3}^2 \chi_{\mathrm{Q}}$ whose temperature dependence was confirmed by elastic constant measurements [17]. Treating the Hamiltonian of Eq. (1) in perturbation theory, one obtains a correction to the free energy density of the form $\delta f \sim \frac{\delta c_u}{2} \langle \varepsilon_{\mathrm{u/v}}^2 \rangle$. Here, a finite expectation value $\langle \varepsilon_{\mathrm{u/v}}^2 \rangle$ might arise either from dynamic zero-point fluctuations of the quadrupolar strain or from static strain disorder [21]. This results in a contribution to the bulk thermal expansion $\delta\beta = \partial_p \partial_T \delta f = -\frac{1}{2}(\partial_p n_{\mathrm{Pr}} g_{\Gamma_3}^2 \langle \varepsilon_{\mathrm{u/v}}^2 \rangle) \partial_T \chi_{\mathrm{Q}}$.

The divergence $\delta\beta \sim 1/T$ originating from $\chi_Q \sim \log(1/T)$ is consistent with the observations in Fig. 4(d).

Hence, dynamic as well as static strain fluctuations can in principle explain the observed singular behavior in β. However, both scenarios also imply a contribution to the specific heat $\delta C_m \sim 1/T$, which so far has not been successfully identified. A possible reason is a small prefactor of δC_m, or, equivalently, a large effective Grüneisen parameter $\delta\Gamma_B = \delta\beta/\delta C_m$ characterizing the hydrostatic pressure dependence of $n_{Pr} g^2_{\Gamma_3} \langle \varepsilon^2_{u/v} \rangle$. This dependence can arise from elastic anharmonicities, e.g., via the elastic coupling $g_{\Gamma_3}(p)$ or, in the case of strain disorder, from a response of $n_{Pr}\langle \varepsilon^2_{u/v} \rangle$ to pressure changes. From Fig. 4(d) we can estimate a lower bound $\Gamma_B > 2.15\ \mathrm{GPa}^{-1}$, and with the isothermal compressibility $\kappa_T \approx 0.01\ \mathrm{GPa}^{-1}$, estimated from elastic constant measurements on $PrIr_2Zn_{20}$ [28], this implies a dimensionless Grüneisen parameter $\delta\Gamma_B\kappa_T$ at least of the order of 200 to be compared with a typical value of 1 for metals [29]. As elastic anharmonicities are in general unlikely to account for such large values, this suggests static strain disorder to be at its origin. Hydrostatic pressure will influence the local strain distribution and might thus affect sensitively the quadrupolar environment of each Pr ions resulting in a large response. Local strain fields were also invoked to explain the temperature and field dependence of the specific heat [5] and the elastic constant [17], respectively. Future nuclear quadrupolar resonance measurements might help clarify this issue.

In this work, we established the symmetrized quadrupolar expansivity, i.e., thermal expansion and magnetostriction, as well as the quadrupolar Grüneisen parameter as a highly sensitive probe to uncover quadrupolar fluctuations. For the example of highly diluted $Y_{1-x}Pr_xIr_2Zn_{20}$ we demonstrated that it gives access to the quadrupolar susceptibility. Our experimental results are in excellent agreement with expectations for the single-impurity quadrupolar Kondo effect and corroborate its emergence in this material. On a more general note, we anticipate the quadrupolar expansivity and quadrupolar Grüneisen parameter to become an important tool also for the investigation of other materials with pronounced quadrupolar correlations; in particular, for materials close to a nematic quantum critical point as discussed for certain cuprate and iron pnictide superconductors [30,31].

Long-term collaboration with R. Küchler as well as helpful discussions with Y. Tokiwa, R. Yamamoto, T. Yanagaisawa, and H. Kusunose are gratefully acknowledged. The work in Augsburg was supported by the German Research Foundation (DFG) via Project No. 107745057 (TRR80). The work in Hiroshima was supported by the Center for Emergent Condensed-Matter Physics (ECMP), Hiroshima University and financially supported by Grants-in-Aid from MEXT/JSPS of Japan [Grants No. JP26707017, No. JP15H05886 (J-Physics), No. JP15KK0169, No. JP18H01182, and No. JP18KK0078]. M.G. is supported by the DFG via Project No. 422213477 (TRR 288, A11).

[1] P. Gegenwart, Q. Si, and F. Steglich, Quantum criticality in heavy fermion metals, Nat. Phys. **4**, 186 (2008).

[2] L. Zhu, M. Garst, A. Rosch, and Q. Si, Universally Diverging Grüneisen Parameter and the Magnetocaloric Effect Close to Quantum Critical Points, Phys. Rev. Lett. **91**, 066404 (2003).

[3] P. Gegenwart, Grüneisen parameter studies on heavy fermion quantum criticality, Rep. Prog. Phys. **79**, 114502 (2016).

[4] T. Onimaru, K. Izawa, K. T. Matsumoto, T. Yoshida, Y. Machida, T. Ikeura, K. Wakiya, K. Umeo, S. Kittaka, K. Araki, T. Sakakibara, and T. Takabatake, Quadrupole-driven non-Fermi-liquid and magnetic-field-induced heavy fermion states in a non-Kramers doublet system, Phys. Rev. B **94**, 075134 (2016).

[5] Y. Yamane, T. Onimaru, K. Wakiya, K. T. Matsumoto, K. Umeo, and T. Takabatake, Single-Site Non-Fermi-Liquid Behaviors in a Diluted $4f^2$ System $Y_{1-x}Pr_xIr_2Zn_{20}$, Phys. Rev. Lett. **121**, 077206 (2018).

[6] K. Matsubayashi, T. Tanaka, A. Sakai, S. Nakatsuji, Y. Kubo, and Y. Uwatoko, Pressure-Induced Heavy Fermion Superconductivity in the Nonmagnetic Quadrupolar System $PrTi_2Al_{20}$, Phys. Rev. Lett. **109**, 187004 (2012).

[7] Y. Shimura, M. Tsujimoto, B. Zeng, L. Balicas, A. Sakai, and S. Nakatsuji, Field-induced quadrupolar quantum criticality in PrV_2Al_{20}, Phys. Rev. B **91**, 241102(R) (2015).

[8] D. L. Cox, Quadrupolar Kondo Effect in Uranium Heavy-Electron Materials?, Phys. Rev. Lett. **59**, 1240 (1987).

[9] D. L. Cox and A. Zawadowski, Exotic Kondo effects in metals: Magnetic ions in a crystalline electric field and tunnelling centres, Adv. Phys. **47**, 599 (1998).

[10] T. Onimaru and H. Kusunose, Exotic quadrupolar phenomena in non-Kramers doublet systems—The cases of PrT_2Zn_{20} (T = Ir, Rh) and PrT_2Al_{20} (T = V, Ti)—, J. Phys. Soc. Jpn. **85**, 082002 (2016).

[11] A. Sakai and S. Nakatsuji, Kondo effects and multipolar order in the cubic $PrTr_2Al_{20}$ (Tr = Ti, V), J. Phys. Soc. Jpn. **80**, 063701 (2011).

[12] M. Tsujimoto, Y. Matsumoto, T. Tomita, A. Sakai, and S. Nakatsuji, Heavy-Fermion Superconductivity in the Quadrupole Ordered State of PrV_2Al_{20}, Phys. Rev. Lett. **113**, 267001 (2014).

[13] A. S. Patri, A. Sakai, S. B. Lee, A. Paramekanti, S. Nakatsuji, and Y. B. Kim, Unveiling hidden multipolar orders with magnetostriction, Nat. Commun. **10**, 4092 (2019).

[14] A. S. Patri and Y. B. Kim, Critical Theory of Non-Fermi Liquid Fixed Point in Multipolar Kondo Problem, Phys. Rev. X **10**, 041021 (2020).

[15] K. Iwasa, H. Kobayashi, T. Onimaru, K. T. Matsumoto, N. Nagasawa, T. Takabatake, S. Ohira-Kawamura, T. Kikuchi, Y. Inamura, and K. Nakajima, Well-defined crystal field splitting schemes and non-Kramers doublet ground states of f electrons in PrT_2Zn_{20} (T = Ir, Rh, and Ru), J. Phys. Soc. Jpn. **82**, 043707 (2013).

[16] T. Onimaru, K. T. Matsumoto, Y. F. Inoue, K. Umeo, T. Sakakibara, Y. Karaki, M. Kubota, and T. Takabatake, Antiferroquadrupolar Ordering in a Pr-Based Superconductor $PrIr_2Zn_{20}$, Phys. Rev. Lett. **106**, 177001 (2011).

[17] T. Yanagisawa, H. Hidaka, H. Amitsuka, S. Zherlitsyn, J. Wosnitza, Y. Yamane, and T. Onimaru, Evidence for the

Single-Site Quadrupolar Kondo Effect in the Dilute Non-Kramers System $Y_{1-x}Pr_xIr_2Zn_{20}$, Phys. Rev. Lett. **123**, 067201 (2019).

[18] M. Zacharias, I. Paul, and M. Garst, Quantum Critical Elasticity, Phys. Rev. Lett. **115**, 025703 (2015).

[19] M. S. Ikeda, J. A. W. Straquadine, A. T. Hristov, T. Worasaran, J. C. Palmstrom, M. Sorensen, P. Walmsley, and I. R. Fisher, AC elastocaloric effect as a probe for thermodynamic signatures of continuous phase transitions, Rev. Sci. Instrum. **90**, 083902 (2019).

[20] R. Küchler, A. Wörl, P. Gegenwart, M. Berben, B. Bryant, and S. Wiedmann, The world's smallest capacitive dilatometer, for high-resolution thermal expansion and magnetostriction in high magnetic fields, Rev. Sci. Instrum. **88**, 083903 (2017).

[21] See Supplemental Material at http://link.aps.org/supplemental/10.1103/PhysRevResearch.4.L022053 for details on the experimental methods; crystal electric field calculations; theory on the volume thermal expansion; data of the longitudinal, transverse, and volume thermal expansion and magnetostriction; and the quadrupole field susceptibility analysis, which includes Refs. [22–26].

[22] Y. Yamane, T. Onimaru, K. Uenishi, K. Wakiya, K. T. Matsumoto, K. Umeo, and T. Takabatake, Impurity quadrupole Kondo ground state in a dilute Pr system $Y_{1-x}Pr_xIr_2Zn_{20}$, Phys. B (Amsterdam. Neth.) **536**, 40 (2018).

[23] Y. Yamane, T. Onimaru, K. Wakiya, K. T. Matsumoto, K. Umeo, and T. Takabatake, Magnetic field effects on the specific heat of a diluted Pr system $Y_{1-x}Pr_xIr_2Zn_{20}$, AIP Adv. **8**, 101338 (2018).

[24] R. Pott and R. Schefzyk, Apparatus for measuring the thermal expansion of solids between 1.5 and 380 K, J. Phys. E: Sci. Instrum. **16**, 444 (1983).

[25] A. Wörl, T. Onimaru, Y. Tokiwa, Y. Yamane, K. T. Matsumoto, T. Takabatake, and P. Gegenwart, Highly anisotropic strain dependencies in $PrIr_2Zn_{20}$, Phys. Rev. B **99**, 081117(R) (2019).

[26] K. Lea, M. Leask, and W. Wolf, The raising of angular momentum degeneracy of f-electron terms by cubic crystal fields, J. Phys. Chem. Solids **23**, 1381 (1962).

[27] R. Küchler, C. Stingl, and P. Gegenwart, A uniaxial stress capacitive dilatometer for high-resolution thermal expansion and magnetostriction under multiextreme conditions, Rev. Sci. Instrum. **87**, 073903 (2016).

[28] I. Ishii, H. Muneshige, Y. Suetomi, T. K. Fujita, T. Onimaru, K. T. Matsumoto, T. Takabatake, K. Araki, M. Akatsu, Y. Nemoto, T. Goto, and T. Suzuki, Antiferro-quadrupolar ordering at the lowest temperature and anisotropic magnetic field–temperature phase diagram in the cage compound $PrIr_2Zn_{20}$, J. Phys. Soc. Jpn. **80**, 093601 (2011).

[29] N. Ashcroft and N. Mermin, *Solid State Physics* (Saunders College Publishing, Philadelphia, 1976), Chap. 25.

[30] N. Auvray, B. Loret, S. Benhabib, M. Cazayous, R. Zhong, J. Schneeloch, G. Gu, A. Forget, D. Colson, I. Paul, A. Sacuto, and Y. Gallais, Nematic fluctuations in the cuprate superconductor $Bi_2Sr_2CaCu_2O_{8+\delta}$, Nat. Commun. **10**, 5209 (2019).

[31] T. Worasaran, M. S. Ikeda, J. C. Palmstrom, J. A. W. Straquadine, S. A. Kivelson, and I. R. Fisher, Nematic quantum criticality in an Fe-based superconductor revealed by strain-tuning, Science **372**, 973 (2021).